Solar Phys (2010) 266: 379–390
DOI 10.1007/s11207-010-9618-0

The Magnetic Field at the Inner Boundary of the Heliosphere Around Solar Minimum

X.P. Zhao · J.T. Hoeksema

Received: 25 March 2010 / Accepted: 21 July 2010 / Published online: 28 August 2010

Abstract STEREO A and B observations of the radial magnetic field between 1 January 2007 and 31 October 2008 show significant evidence that in the heliosphere, the ambient radial magnetic field component with any dynamic effects removed is uniformly distributed. Based on this monopolar nature of the ambient heliospheric field we find that the surface beyond which the magnetic fields are in the monopolar configuration must be spherical, and this spherical surface can be defined as the inner boundary of the heliosphere that separates the monopole-dominated heliospheric magnetic field from the multipole-dominated coronal magnetic field. By using the radial variation of the coronal helmet streamers belts and the horizontal current – current sheet – source surface model we find that the spherical inner boundary of the heliosphere should be located around 14 solar radii near solar minimum phase.

Keywords Heliosphere · Heliospheric base · Sun: corona · Sun: magnetic field

1. Introduction

The heliosphere is the immense magnetic bubble around the Sun through which the solar wind extends and through which the Sun exerts a magnetic influence. Its outer boundary is called the heliospheric pause, or simply the "heliopause", which can be easily defined using the distinguished boundary layer existing between the heliosphere and the surrounding interstellar medium, *i.e.*, the discontinuity where the outgoing solar wind meets the incoming plasma from interstellar space. The location and shape of the heliopause can be quantitatively estimated, on the basis of the balance between the interstellar medium and solar wind pressures (Axford (1990) and references therein).

Unlike the heliopause, no any discontinuity exists between the outgoing corona and the outgoing heliosphere. It is harder to define the location, shape, and characteristics of the inner boundary of the heliosphere than to define the outer boundary. For simplicity, the inner

X.P. Zhao (✉) · J.T. Hoeksema
W. W. Hansen Experimental Physics Laboratory, Stanford University, Stanford, CA 94305-4085, USA
e-mail: xuepu@sun.stanford.edu

boundary of the heliosphere will be called the heliospheric base or "heliobase", corresponding to the heliospheric pause or heliopause in what follows.

Although there is no strict definition of the heliobase in the literature, the heliobase is generally assumed to be a spherical surface that separates the super-Alfvén solar wind from the sub-Alfvénic coronal expansion in various heliospheric MHD models (see *e.g.* Odstrcil, Riley, and Zhao, 2004). There is no effective way in literature to determine the location of the spherical heliobase. It is usually assumed that the heliobase is located around 10 – 20 solar radii or 0.1 AU, and the magnetic field on the heliobase is the same as the source surface of the potential field – source surface (PFSS) or coronal MHD models.

However, in situ observations of the heliospheric magnetic field (HMF) by the Ulysses, STEREO spacecraft and other satellites have shown that the ambient radial HMF is definitely latitude independent, and probably longitude independent as well (Owens *et al.* (2008a) and references therein), implying that the magnetic field on the heliobase is different from the source surface field of the PFSS model.

It has been shown that the success of MHD simulations of CME propagation in the inner heliosphere depends heavily on the initial condition of the inner heliosphere, as well as on the CME input parameters (Owens *et al.*, 2008b). More accurately specifying the inner boundary condition of heliospheric MHD models may improve the MHD simulations of CME propagation in the inner heliosphere and the space weather forecasting.

This work tries to find out the magnetic characteristics in the solar atmosphere that can be used to distinguish the corona from the heliosphere, and it can in turn be used to define the heliobase. This work also provides ways to more accurately determine the location and shape of the heliobase.

In what follows we first examine the radial variation of magnetic field directions in the outward expanding corona, and determine where is the highest radial Alfvén critical points around the solar minimum on the basis of the radial variation of the coronal helmet streamer belt observed by SOHO/LASCO C2 and C3 (Brueckner *et al.*, 1995); we then confirm the uniformity of the ambient radial HMF using the radial HMF component observed by STEREO A and B spacecraft (Acuña *et al.*, 2007), and strictly define the characteristics and the shape of the heliobase; finally we determine the location of the heliobase using the horizontal current – current sheet – source surface (HCCSSS) model (Zhao and Hoeksema, 1995; Zhao, Hoeksema, and Rich, 2002).

2. Determination of the Highest Radial Alfvén Critical Point

The hot coronal and heliospheric plasma has an extremely high electrical conductivity and is pervaded by a frozen-in magnetic field of solar origin. Therefore, stream lines of plasma flow coincide with magnetic field lines in the expanding corona. The nonradialness of magnetic field lines and stream lines are determined by the interaction between the magnetic field and expanding plasma, specifically, by the magnetic stress and plasma inertia. In the inner corona below the Alfvén critical points, the magnetic stress dominates the interaction. The coronal magnetic field is largely dipole-like around the minimum phase of solar activity. The gradient of radial field strength in latitude, with stronger field at higher magnetic latitude, bends stream lines from the radial direction toward the magnetic equator. As shown in recent solar eclipse and coronagraph images, the nonradial ray-like structures in open field regions and the nonradial striations beyond coronal streamers suggest that many coronal magnetic field lines are nonradial around 2.5 $R_{\odot}$, except near the magnetic equator (see, for example, http://esthersim15.files.wordpress.com/2008/06/bla.jpg for the 1998 total

eclipse and Figure 1 of Guhathakurta and Fisher (1995) for a coronagraph image). However, in the corona beyond the Alfvén critical point, it is the inertia of radially accelerated plasma flow that dominates the magnetic field-plasma interaction (note: the stream interaction between radially accelerated plasma streams in the corona is certainly not significant and can be neglected). All nonradial structures, which are supposed to be along nonradial field lines, change their direction and become asymptotically radial at different heliocentric distances.

It has been shown that solar wind solutions of coronal expansion models that include a magnetic force must pass continuously through three consecutive critical points associated with the sound speed, the Alfvén speed, and the radial Alfvén speed (Hundhausen, 1972). The analytic simulation of the interaction between the isothermal solar wind and dipolar magnetic field (Pneuman and Kopp, 1971) specifically showed that both sonic critical points and Alfvén critical points are not spherical-symmetrically distributed: the lowest (highest) sonic critical point occurs in the pole (equator), and the lowest (highest) Alfvén critical point occurs in the equator (pole), respectively. In addition, the lowest sonic critical point is higher than the lowest Alfvén critical point. Thus the heliobase should be set at or beyond the highest radial Alfvén critical point but the shape of the heliobase is certainly different from the surface of Alfvén critical points.

Where is the highest radial Alfvén critical point located?

The nonradial striations beyond cusp points of helmet streamers are believed to be formed by the scattering electrons in the plasma sheet surrounding the heliospheric current sheet, *i.e.*, in the boundary layer between solar wind streams with opposite magnetic polarity.

As the heliocentric distance increases from the inner corona to the outer corona, the direction of each striation becomes increasingly radial. Therefore, the latitudinal extent of coronal helmet streamer belts in the outer corona is expected to be smaller than that in the inner corona around solar minimum, and the shape of helmet streamer belts is gradually flattening toward the equator. The heliocentric distance beyond which the shape of the helmet streamer belts becomes height independent should be an indication of the height beyond which all magnetic fields are purely radial.

Figure 1 displays the SOHO/LASCO Carrington maps of the corona for Carrington rotation (CR) 1922 in May, 1997. The left (right) column is constructed using east (west) limb observations of coronagraphs C2 and C3, respectively. The topology of the streamer belts indeed shows slight radial variation, gradually flattening toward the equator as the heliocentric distance increases from 2.5 to 20 solar radii. This radial variation of the helmet streamer belt is governed by the inertia of radially accelerating plasma flow.

Superposed on Figure 1 are magnetic neutral lines (solid dark lines) computed using the HCCSSS model with the optimum set of parameter values: $a = 0.2\ R_\odot$, $R\mathrm{cp} = 2.25\ R_\odot$ and $R\mathrm{ss} = 14.0\ R_\odot$ (see Zhao, Hoeksema, and Rich (2002) for the definition of the parameters a, $R\mathrm{cp}$ and $R\mathrm{ss}$). The neutral lines in the bottom panels are calculated at $r = 14\ R_\odot$.

There is a wispy, arc-like feature near Carrington longitude 270° that curves away from the equator. Wang (1997) explained such features of bright streamers seen in the coronagraph images as the result of line-of-sight viewing along a convoluted or "folded" heliospheric plasma sheet of uniform density centered at the magnetic neutral line. The arc-like features represent a projection effect, whereby individual structures move to higher (lower) apparent latitudes as they rotate away from (toward) the plane of the sky, respectively. Because of the tilt of the Sun's rotation axis relative to the sky plane, the arcs exhibit an east – west asymmetry with opposing directions in the northern and southern hemisphere and in the east and west limb maps.

Figures 2 and 3 are like Figure 1 but show Carrington rotations 1936 and 1947 (May 1998 and March 1999, respectively). The bright structures farther from minimum are more

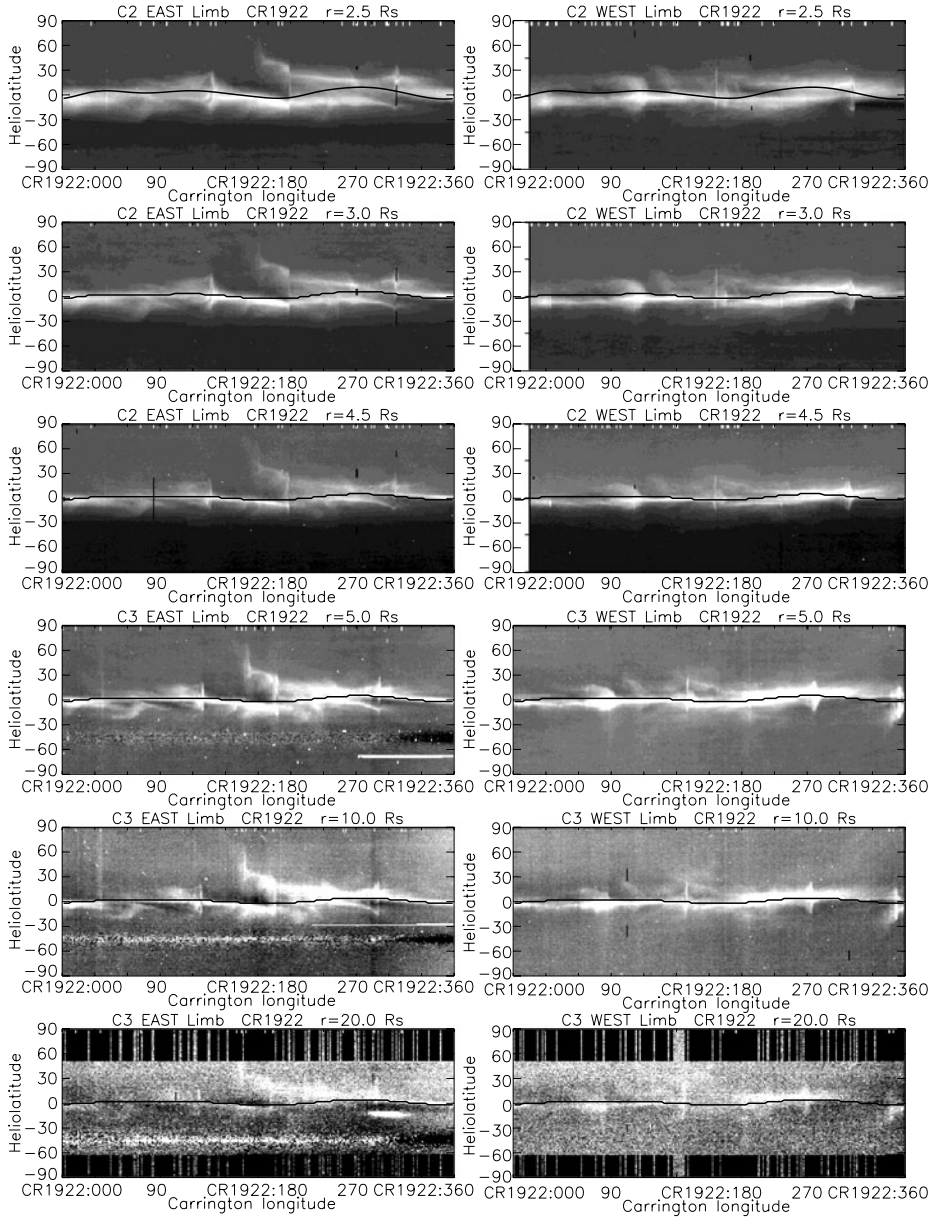

Figure 1 Coronal streamer belts (bright structures) and magnetic neutral lines (dark lines) of CR 1922 at various heights.

complicated than CR1922. Almost all arc-like features are matched by the segments of neutral lines that lie nearly parallel to solar equator, though there appears to be no single, stable current sheet being viewed alternately edge-on and then flat-on. The match suggests the existence of the neutral lines. The vertical bright features in the maps (*e.g.* at CR1936:230° in Figure 2) are caused by coronal mass ejections.

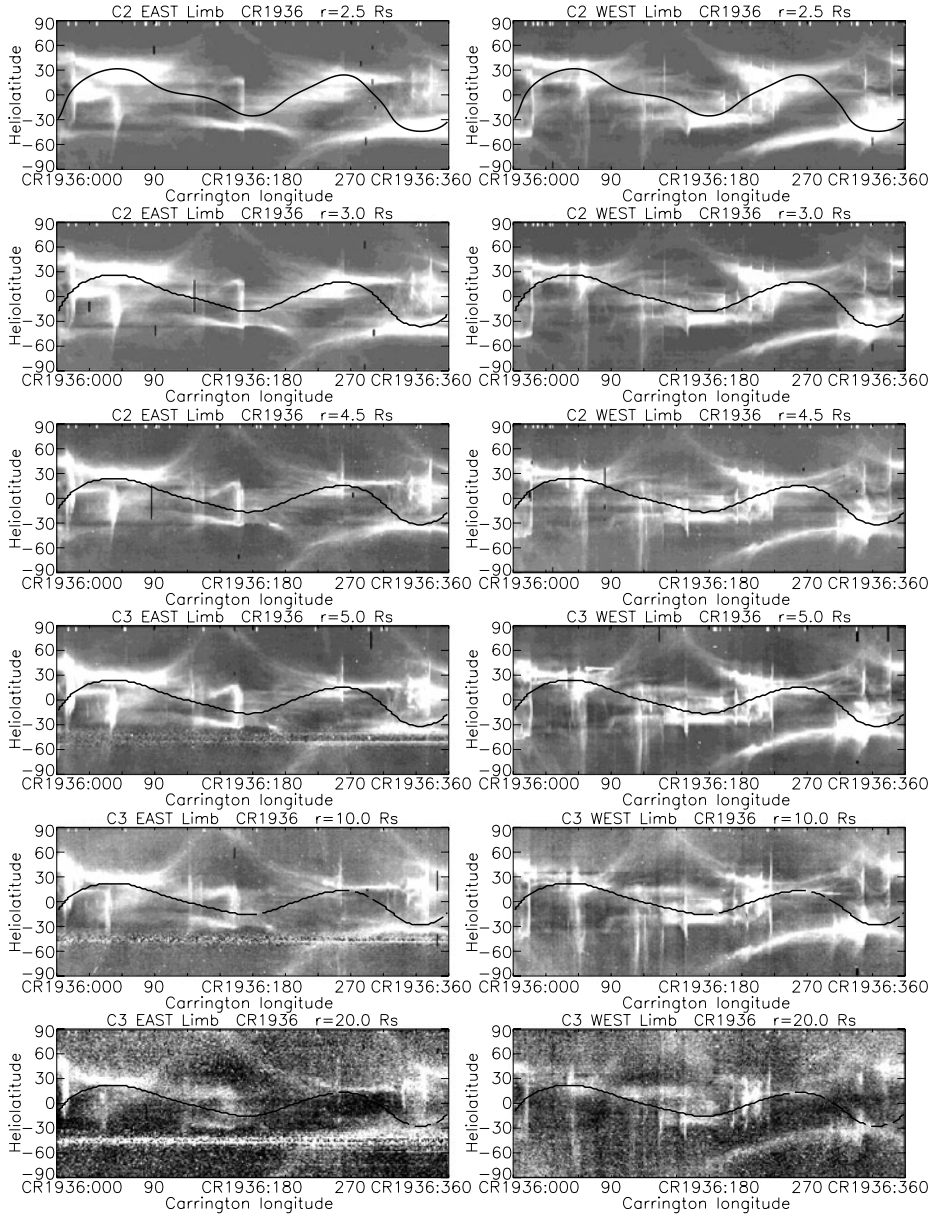

Figure 2 The same as Figure 1, but for CR1936. See text for the cause of the wispy, arc-like features curved away from the equator.

Figure 4 shows the radial variation in the shape of the computed magnetic neutral lines for CR1922, CR1936 and CR1947 that match the observed helmet streamer belts. The black solid, red dotted, green dotted, and blue dashed lines denote, respectively, the neutral line calculated at 2.5, 5.0, 10.0 and 14.0 solar radii. The radial variation in both minimum and ascending activity phases occurs mainly in the latitudinal direction, implying that different

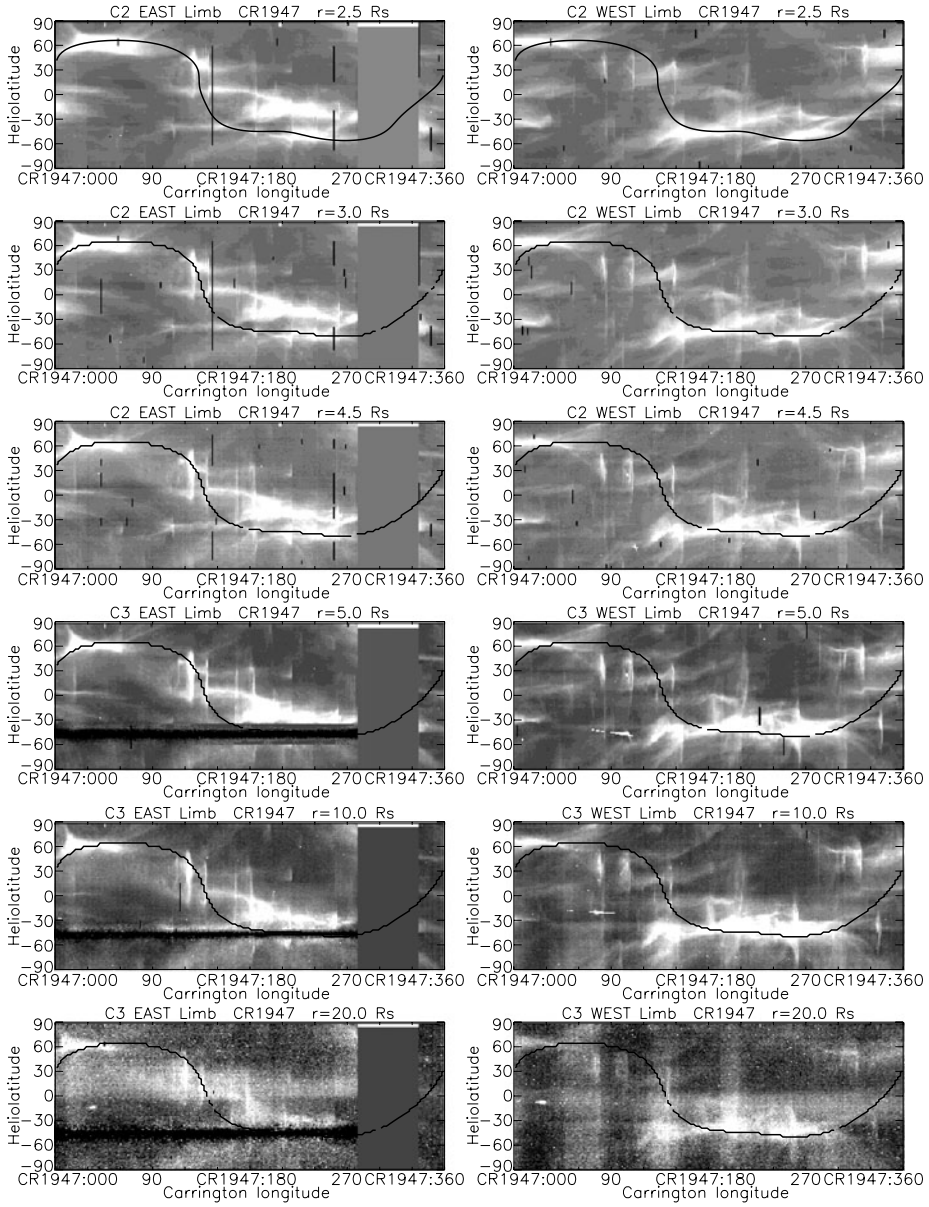

Figure 3 The same as Figure 1, but for CR1947.

helmet streamers become radial at different heliocentric distances. The intersection points of all four curves are the lowest radial Alfvén critical point located at 2.5 solar radii, and the intersection points of green and blue curves are the radial Alfvén critical points located at 10 solar radii. The point where only the blue curve reaches the lowest latitude denote the highest radial Alfvén critical point. Obviously, the difference between the neutral

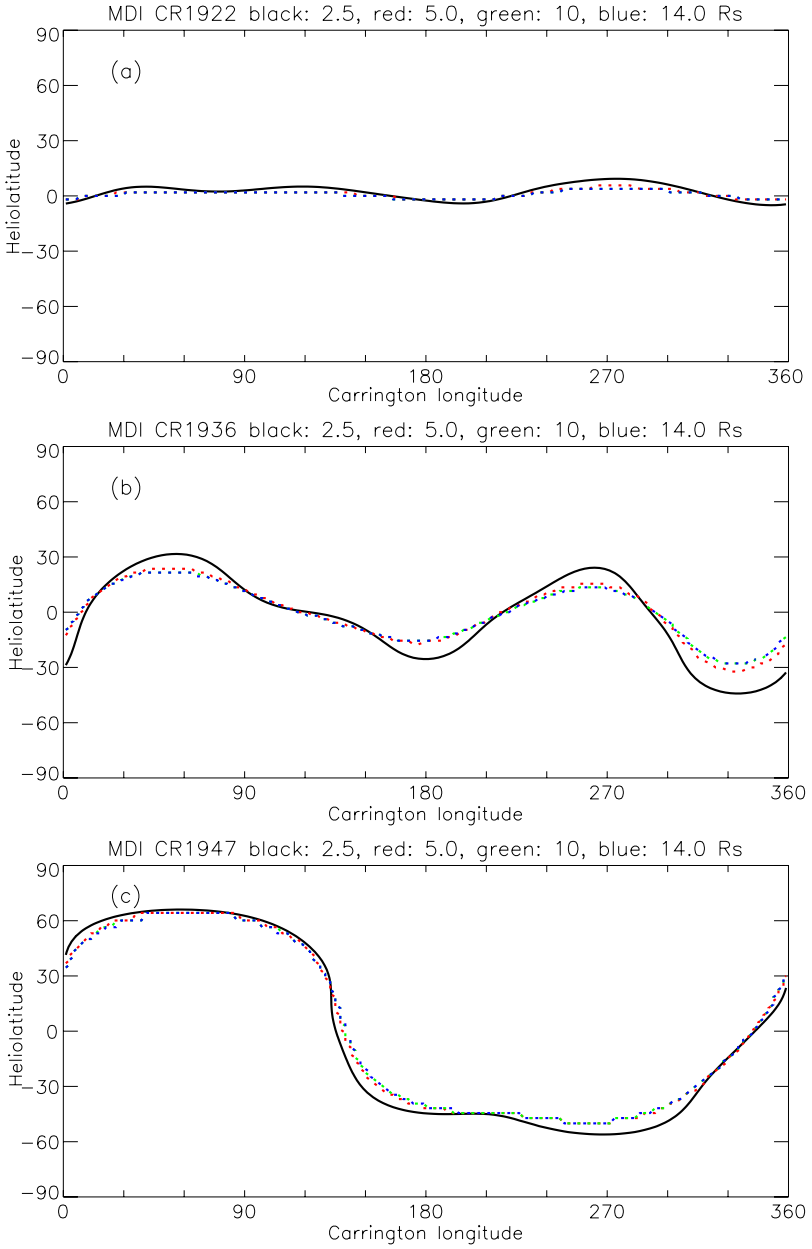

Figure 4 Radial variation of the magnetic neutral lines computed using the HCCSSS model applied to MDI magnetic synoptic maps for (a) CR 1922, (b) CR 1936, and (c) CR 1947, respectively.

lines at 10 $R_\odot$ and 14 $R_\odot$ is hard to distinguish, suggesting that the method provides only an approximate estimate of the heliocentric distance of the highest radial Alfvén critical point.

3. The Monopolar Nature of the Ambient Radial HMF and the Definition of the Heliobase

The radial field at the heliobase extends radially and decreases predictably in the inner heliosphere. The radial HMF component measured by spacecraft contains information about the field near the heliospheric base. However, the HMF measured by spacecraft at various heliocentric distances differs from the original magnetic field, being subject to various dynamic effects such as large-amplitude Alfvén fluctuations, stream – stream interactions, and coronal mass ejections (Smith and Balogh (1995) and references therein).

In order to determine the ambient radial HMF component without the dynamic effects, the hourly radial HMF component measured by spacecraft at various distances is first normalized to 1 AU and then averaged over 24 hours to smooth out the effects of large-amplitude Alfvén fluctuations and various noise sources. Finally, the daily radial HMF component is running-averaged over one or three solar rotations to filter out the effects of longitudinal structures, stream – stream interactions, and coronal mass ejections.

Based on the measurements at Ulysses as it traveled between near the solar equator and the poles, the ambient radial HMF component has been shown to be approximately constant and latitude independent (Smith and Balogh, 1995, 2003). The recent analysis of multiple single-point in situ measurements of the radial HMF component shows that there are no obvious trends in either the latitude or the longitude scatter plots (see Figure 5 of Owens *et al.*, 2008a). This result not only confirms that the ambient radial HMF component without dynamic effects is latitude independent, but it also suggests that it is statistically longitude independent as well (Owens *et al.*, 2008a).

From 1 January 2007 to 31 October 2008, the longitudinal separation between the STEREO A and B spacecraft increases from 0.5° (*i.e.*, the STEREO B is located nearly at the same position of the STEREO A) to 80.6° (see the blue number near the upper axis of the bottom panel in Figure 5). The radial HMF component measured simultaneously by the STEREO A and B spacecraft in the period of time provides an unprecedented opportunity to examine the dependence of the ambient radial HMF component on the longitude. The top and bottom panels of Figure 5 display, respectively, the daily radial HMF component and the three-rotation average of the daily HMF strength. The thick blue lines in the bottom panel denotes the difference of the three-rotation averages between STEREO A and B. The differences at all longitudinal separations up to 80.6° are the same as the difference at 0.5°. This implies that the ambient radial HMF component is indeed longitude independent.

This means that the magnetic field on the heliobase should be a uniform radial field. Ignoring polarity, this is the configuration of the monopolar field. Since the monopolar field decreases uniformly as the heliocentric distance, r, increases according to $1/r^2$, the surface where magnetic fields distributes uniformly must be a spherical surface. Therefore, we define the heliobase as a spherical surface where magnetic fields start to distribute uniformly. This is the boundary layer separating the multipolar coronal field from the monopolar heliospheric field.

4. Determination of the Heliocentric Distance of the Heliobase

The uniform radial HMF, the monopolar field, is associated with the sheet current in the heliospheric current sheet. The monopole here is a mathematical description of the contribution of the sheet current to the magnetic field (to avoid confusing cause and effect, it is correct to say that a uniform radial field which reverses sign at the magnetic equator gives rise to

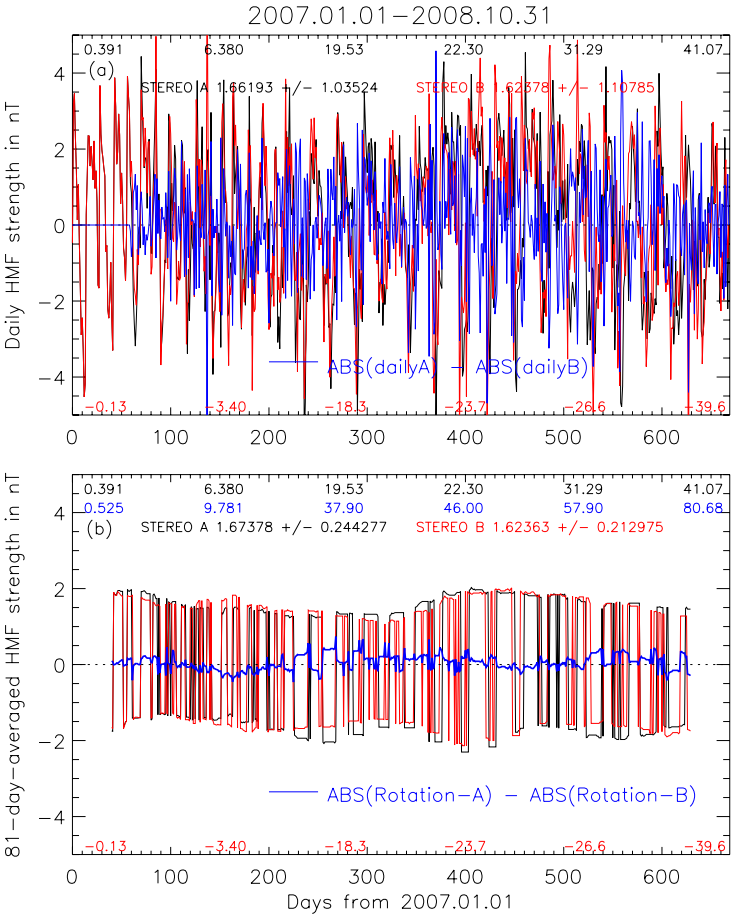

Figure 5 (a) The time variation of the daily-averaged radial HMF component observed by STEREO A and B normalized to 1 AU. (b) A three-rotation running average of the daily HMF averages. The black and red numbers near the upper and lower axes denote the longitude of A and B relative to the Earth. The blue numbers denote the angular distance between A and B.

the sheet current (Smith and Balogh, 1995)). Thus the uniform radial field is supposed to correspond to the virtual monopole and can be reproduced when the virtual monopole contribution arising from the heliospheric current sheet becomes dominant. The current sheet model with an infinite outer boundary condition has shown that the monopolar field occurs at larger heliocentric distance, where the virtual monopole contribution becomes dominant (Wang, 1996).

By introducing the source surface in coronal models, the contribution of multipoles to the magnetic field is suppressed, and the contribution of the monopole is increased. The monopolar field predicted by the HCCSSS model is expected to occur at a heliocentric distance lower than that of the current sheet model with an infinite outer boundary condition.

As shown in Section 2, the highest radial Alfvén critical point around solar minimum may be located between 10 and 14 $R_{\odot}$, where both the effect of solar rotation can be neglected and stream – stream interactions are unimportant. The characteristic uniform radial field, as

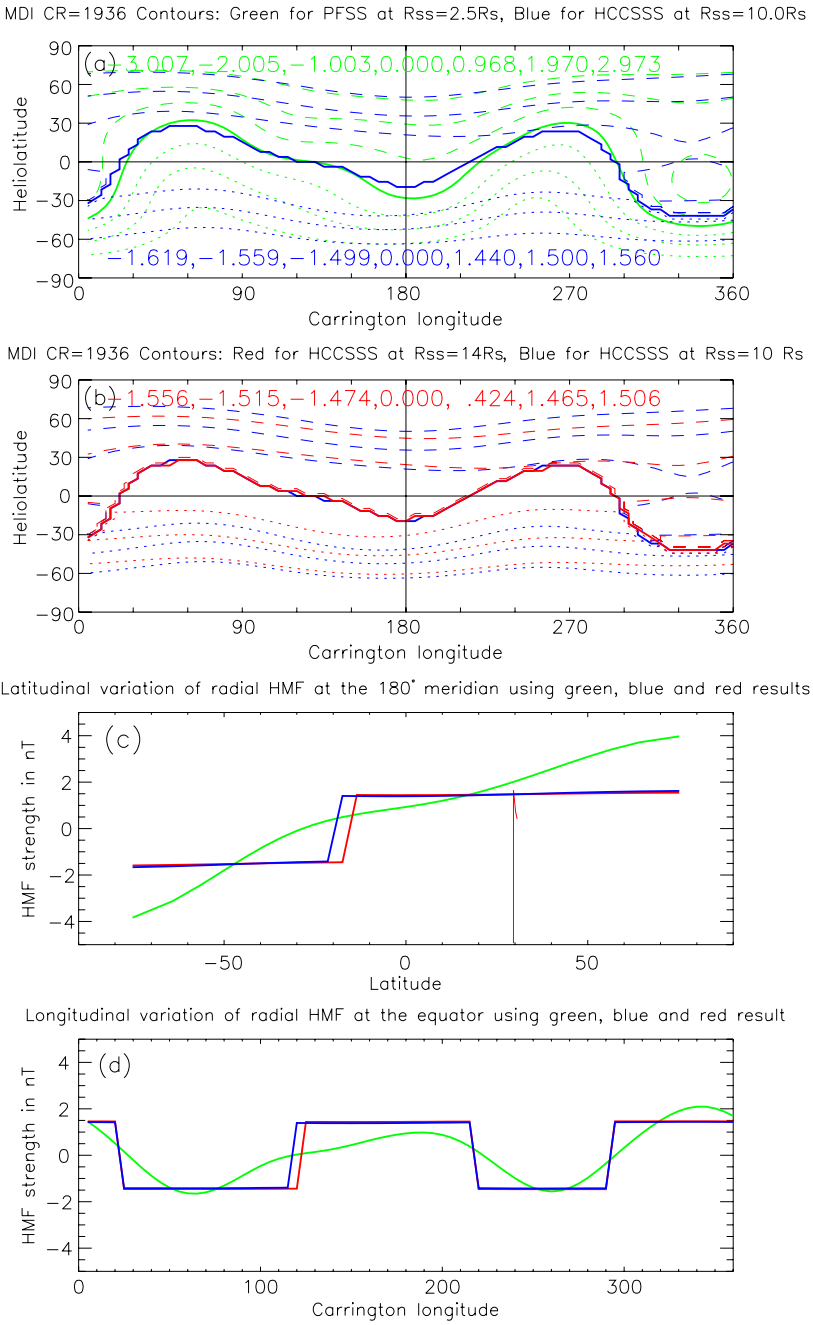

Figure 6 The radial HMF component inferred on the basis of PFSS (green at $Rss = 2.5\ R_{\odot}$) and HCCSSS models (blue at $Rss = 10\ R_{\odot}$ and red at $Rss = 14\ R_{\odot}$). The numbers for contours are field strengths normalized to 1 AU. See the discussion in Section 4 for Figure 6.

evidenced in the heliosphere, can be helpful to more accurately find the radial location of the heliospheric base.

To examine which heliocentric distance, 10 or 14 $R_\odot$, is the better candidate for the location of the heliospheric base, we apply the HCCSSS model to the MDI synoptic maps with the source surface at 10 $R_\odot$ and 14 $R_\odot$, respectively. In order to compare the source surface field of the HCCSSS model with that of the PFSS model having a source surface located at 2.5 $R_\odot$, Figure 6 displays the radial field calculated at the source surface of the PFSS model along with the HCCSSS models. The numbers for contours in Figures 6a and 6b denote the field strength normalized to 1 AU. Figure 6a compares the distribution of field strengths calculated at 2.5 $R_\odot$ using the PFSS model (green) and at 10 $R_\odot$ using the HCCSSS model (blue). The thick curves denote the neutral lines, and dotted and dashed contours are for negative and positive polarities, respectively. The difference between adjacent green contours is ≈ 1.0 nT, but the difference between adjacent blue contours is ≈ 0.07 nT much more consistent with a uniform field strength.

Red contours in Figure 6b show the distribution of the field strength calculated on the source surface of the HCCSSS model at 14 $R_\odot$. The blue contours are the same as in Figure 6a. The difference between adjacent red contours is ≈ 0.04 nT, less than that between blue contours, showing that 14 $R_\odot$ is a better candidate for the location of the heliospheric base.

Figures 6c and 6d show the distribution of field strengths along the vertical (horizontal) dark line in Figures 6a and 6b, *i.e.*, along the 180° meridian (the equator). The red, green and blue in Figures 6c and 6d are for the same case as in Figures 6a and 6b. The red, blue and green lines in Figures 6c and 6d show how the radial field strength distribution evolves from non-uniform to nearly uniform as the heliocentric distance increases from 2.5 $R_\odot$ to 14 $R_\odot$.

5. Summary and Discussion

(1) Based on the radial evolution of the direction of coronal magnetic field we show that the coronal helmet streamer belts observed at several heights by SOHO/LASCO, together with the source surface field of the HCCSSS model, can be used to find the heliocentric distance of the lowest and highest Alfvén critical point. The highest Alfvén critical point around solar minimum is located between 10 and 14 solar radii.

(2) The *in situ* observations of the radial HMF component by STEREO A and B confirm Owens' suggestion (Owens *et al.*, 2008a) that the ambient radial HMF component without any dynamic effects is uniformly distributed. It implies that the magnetic field on the heliobase must be in monopolar configuration.

(3) Based on the monopolar nature of the ambient HMF, the heliobase can be strictly defined as a spherical surface beyond which the magnetic field is distributed uniformly. This inner boundary layer of the heliosphere separates the monopolar heliospheric field from the multipolar coronal magnetic field.

(4) The source surface field of the HCCSSS model at 14 $R_\odot$ matches the uniform field better than at 10 $R_\odot$, showing the heliocentric distance of 14 $R_\odot$ is the better candidate location of the heliospheric base.

(5) The approach used in the present paper to find out the highest radial Alfvén critical point and to determine the location of the heliobase can be extended to other solar activity phases. Since the HCCSSS model can be used to reproduce the radial variation of coronal streamer belts and the monopolar field, the HCCSSS model applied to a specific synoptic

map may provide the inner boundary condition of the heliospheric MHD models for this specific period of time. This inner boundary condition may more accurately characterize Sun's magnetic influence on the heliosphere. The new input may be able to improve the simulation of CME propagation in the inner heliosphere and the space weather forecasting.

Acknowledgements We thank Prof. Y.C. Whang and Dr. Keiji Hayashi for helpful comments and suggestions. We are grateful to SOHO/LASCO team, and STEREO team for the data used in the work. This work is supported by NASA grants NAGW 2502 and NAG5-3077, by NSF grant ATM9400298.

References

Acuña, M.H., Curtis, D., Scheifele, J.L., Russell, C.T., Schroeder, P., Szabo, A., Luhmann, J.G.: 2007, *Space Sci. Rev.* **136**, 203.

Axford, W.I.: 1990, In: Grzedzielski, S., Page, D.E. (ed.) *Physics of the Outer Heliosphere*, Pergamon Press, Oxford, 7.

Brueckner, G.E., Howard, R.A., Koomen, M.J., Korendyke, C.M., Michels, D.J., Moses, J.D., *et al.*: 1995, *Solar Phys.* **162**, 357.

Guhathakurta, M., Fisher, R.R.: 1995, *Geophys. Res. Lett.* **22**, 1841.

Hundhausen, A.J.: 1972, *Solar Wind and Coronal Expansion*, Springer, New York, 66.

Odstrcil, D., Riley, P., Zhao, X.P.: 2004, *J. Geophys. Res.* **109**, A02116.

Owens, M.J., Arge, C.N., Crooker, N.U., Schwadron, N.A., Horbury, T.S.: 2008a, *J. Geophys. Res.* **113**, A12103.

Owens, M.J., Spence, H.E., McGregor, S., Hughes, W.J., Quinn, J.M., Arge, C.N., Riley, P., Linker, J., Odstrcil, D.: 2008b, *Space Weather J.* **6**, S08001.

Pneuman, G.W., Kopp, R.A.: 1971, *Solar Phys.* **18**, 258.

Smith, E.J., Balogh, A.: 1995, *Geophys. Res. Lett.* **22**, 3317.

Smith, E.J., Balogh, A.: 2003, In: Velli, M., Bruno, R., Malara, F. (eds.) *Solar Wind Ten, AIP Conf. Proc.* **679**, 67.

Wang, Y.-M.: 1996, *Astrophys. J. Lett.* **119**, 456.

Wang, Y.-M.: 1997, *Astrophys. J.* **485**, 875.

Zhao, X.P., Hoeksema, J.T.: 1995, *J. Geophys. Res.* **100**, 19.

Zhao, X.P., Hoeksema, J.T., Rich, N.B.: 2002, *Adv. Space Res.* **29**, 411.